Accepted Manuscript

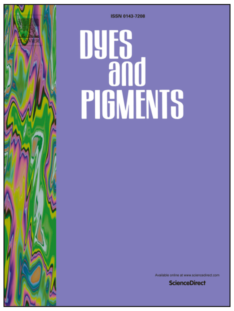

Synthesis and photophysical properties of new perylene bisimide derivatives for application as emitting materials in OLEDs

Marek Matussek, Michał Filapek, Paweł Gancarz, Stanisław Krompiec, Jan Grzegorz Małecki, Sonia Kotowicz, Mariola Siwy, Sebastian Maćkowski, Anna Chrobok, Ewa Schab-Balcerzak, Aneta Słodek

PII: S0143-7208(18)31275-0

DOI: 10.1016/j.dyepig.2018.07.006

Reference: DYPI 6860

To appear in: *Dyes and Pigments*

Received Date: 7 June 2018

Revised Date: 2 July 2018

Accepted Date: 2 July 2018

Please cite this article as: Matussek M, Filapek Michał, Gancarz Paweł, Krompiec Stanisł, Grzegorz Małecki J, Kotowicz S, Siwy M, Maćkowski S, Chrobok A, Schab-Balcerzak E, Słodek A, Synthesis and photophysical properties of new perylene bisimide derivatives for application as emitting materials in OLEDs, *Dyes and Pigments* (2018), doi: 10.1016/j.dyepig.2018.07.006.

Synthesis and photophysical properties of new perylene bisimide derivatives for application as emitting materials in OLEDs

Marek Matussek[1], Michał Filapek[1], Paweł Gancarz[1], Stanisław Krompiec[1], Jan Grzegorz Małecki[1], Sonia Kotowicz[1], Mariola Siwy[2], Sebastian Maćkowski[3], Anna Chrobok[4], Ewa Schab-Balcerzak[1,2*], Aneta Słodek[1*]

[1] *Institute of Chemistry, University of Silesia, 9 Szkolna Str., 40-006 Katowice, Poland*
[2] *Centre of Polymer and Carbon Materials, Polish Academy of Sciences, 34 M. Curie-Sklodowska Str., 41-819 Zabrze, Poland*
[3] *Institute of Physics, Faculty of Physics, Astronomy and Informatics, Nicolaus Copernicus University, 5 Grudziadzka Str., 87-100 Torun, Poland*
[4] *Department of Chemical Organic Technology and Petrochemistry, Silesian University of Technology, Gliwice, Krzywoustego 4, 44-100, Poland*

[*]corresponding authors, E-mail address: ebalcerzak@cmpw-pan.edu.pl (E. Schab-Balcerzak), a.slodek@wp.pl (A. Slodek)

Abstract

Three novel perylene diimide derivatives with bulky aromatic moieties (fluorene, carbazolyl-fluorene, and anthracyl-fluorene) connected via triple bonds with perylene core were successfully designed and synthesized. The chemical structure of prepared compounds was confirmed by ^{1}H and ^{13}C NMR and mass spectrometry. Their optimized ground-state geometry and frontier molecular orbitals were theoretically estimated based on density functional theory. The compounds undergo the reversible electrochemical reduction process and exhibit very low energy band gaps (1.56-1.98 eV) being promising for electronic applications. They also display excellent solubility, high thermal stability and luminescence in solution and in the solid state as a film in the red spectral region. The highest photoluminescence quantum yield (79 % in solution and 28 % in the film) was found for perylene diimide bearing fluorene unit. All molecules showed the ability for light emission under an applied voltage. The fabricated diodes with structure ITO/PEDOT:PSS/compound/Al exhibited electroluminescence with maximum emission band located between 685 and 732 nm. The most intense electroluminescence, which was additionally plasmonically enhanced by incorporating silver nanowires, was observed for the device based on molecules with anthracene structure.

Keywords*:* perylene bisimide, fluorene, carbazole, anthracene, fluorescence, organic electronics

Graphical abstract

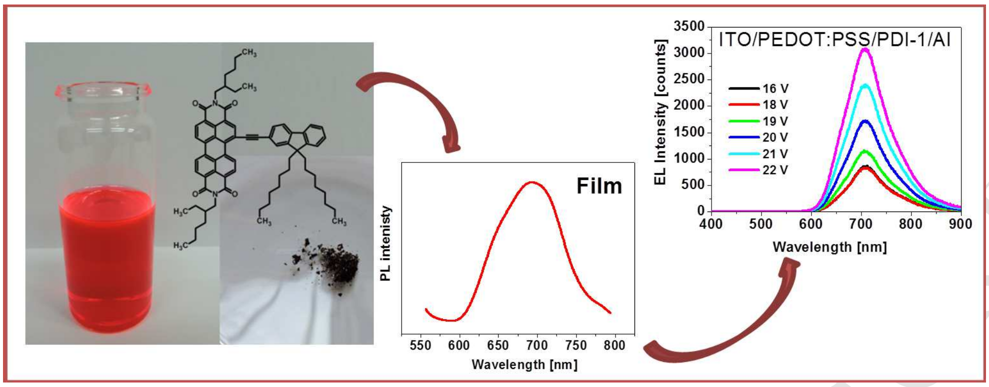

1. Introduction

Perylene-3,4,9,10-tetracarboxylic acid diimides (Perylene bisimides, PDIs) is a class of aromatic compounds consisting of perylene core scaffold substituted by imide groups at *peri*-3,4 and 9,10 positions. The imide groups with well-defined electron-accepting properties attached to π-rich perylene core create a donor-acceptor system (D-A). The rigid structure of highly π-conjugated PDI molecule exhibit appealing electrochemical and spectral properties being used as stable organic semiconductors of n-type [1-4]. They are characterized by high electronic affinity ($E_{ea} \approx -4.0$ eV) and good mobility of negative charges in the solid state (10^{-3} - 10^{1} cm^2/Vs) [5,6], being thus favorably predestined for applications in the area of organic electronics. Moreover, perylene bisimides exhibit strong absorption in the visible region, intense luminescence, and external high thermal and chemical (oxidative) stability [7-9]. However, the PDIs due to their flat structure tend to aggregate in the solid state as a result of π-π interactions [10-12]. Modification of PDIs structure allows to obtain materials with the desired physicochemical properties and to eliminate unfavorable intramolecular interactions, which cause fluorescence quenching. The substitution of the nitrogen atom in PDIs by aliphatic [13,14] and aryl [15,16] motifs allows - in a relatively easy and effective way - to increase their solubility, and strongly inhibited the aggregation in the concentrated solution [17]. The PDI with bulky terminal 2,4-dimethylpent-3-yl substituents showed strong fluorescence not only in the concentrated solution but also in the solid state with the fluorescence quantum yield nearly 100% [18]. Moreover, modification of the PDI core by substitution at 1,6,7 and 12- positions (bay-region) increases the steric strain between naphthalene motifs and, as a consequence, leads to a twist of the perylene core and disturbance of flat structure, which reduces the intermolecular interactions [19-21]. The PDI compounds substituted in the bay region by naphthalene and acenaphthalene moieties were successfully applied as emissive layers in OLED devices. OLED device based on PDI with acenaphthalene units exhibited the best efficiency in the red spectral region (emission at 693 nm, CIE x = 0.69, y = 0.29) described up to now in the literature [20]. The introduction of azaborine into bay position of PDI allowed to obtain the fluorescence quantum yield of 81% notwithstanding the constructed OLED devices with increase of doping ratio of azaborazine-annulated perylene diimide have shown a decrease of the external quantum efficiency (EQE) even to 0.05% assigned to the aggregation induced quenching (AIQ) process [21]. The simple OLED devices composed of layer of dendronized perylene derivatives with the external quantum efficiency above 0.1% and red emission at 650 nm were reported [22]. The appealing physicochemical properties of perylene bisimides, including unique electrical properties and relatively easy and effective PDI structure modification routes, make the described compounds and their derivatives highly attractive for potential use on the organic electronics substrate, including in particular organic light-emitting diodes (OLEDs) [20-22], organic field-effect transistors (OFETs) [23,24], organic photovoltaic cells (OPVs) [25-27], dye lasers [28], sensors [29], and optical power limiters [30].

Here, we report on the synthesis and photophysical characterization of three perylene diimides (**PDIs**) connected *via* triple bonds (C≡C) with bulky aromatic rings (fluorene (**PDI1**), carbazolyl-fluorene (**PDI2**), and anthracyl-fluorene (**PDI3**)) in the bay position, and substituted at N positions by 2-ethylhexyl group. The presence of bulky substituents in PDIs molecules significantly enhances their solubility and inhibits the intermolecular interaction and aggregation. We demonstrate that the novel PDI derivatives are promising candidates for deep red emissive OLEDs.

2. Experimental

2.1 Materials

All reagents were of analytical reagent grade, and were used without further purification. Solvents were distilled by using standard methods and purged with argon before use.

Column chromatography was carried out on Merck silica gel. Thin-layer chromatography (TLC) was performed on silica gel (Merck TLC Silica Gel 60). The key intermediates **1-13** and ethynyl derivatives (**Et-1 – Et-3)** were synthesized according to the well-known procedures with minor modifications, and characterized by ^{1}H NMR and ^{13}C NMR spectroscopic analysis (see Supplementary Information for details). Poly[3,4-(ethylenedioxy)thiophene]:poly-(styrenesulfonate) (PEDOT:PSS) (0.1–1.0 S/cm) and substrates with pixilated ITO anodes were supplied by Ossila.

2.2 Synthesis and characterization

General Sonogashira cross-coupling procedure for perylene bisimide derivatives (PDI1–PDI3)

A solution of **13** (100 mg, 0.138 mmol) in 50 mL degassed TEA was stirred and bubbled with argon for 20 min. After this time, Pd(PPh$_3$)$_4$ (16 mg, 10%-mol), and CuI (3 mg, 10%-mol) were added, and the resulting mixture was bubbled with argon for another 10 min. **Et-1** (69 mg, 0.166 mmol, 1.2 eq), **Et-2** (96 mg, 0.166 mmol, 1.2 eq) or **Et-3** (102 mg, 0.166 mmol, 1.2 eq) in 10 mL TEA was then injected through the septum, and the mixture was stirred at 80 °C for 24h. The resulting mixture was filtered and filtration was evaporated under reduced pressure. After removal of the solvent, the residue was purified by column chromatography giving target compounds (**PDI1–PDI3**).

1-(9,9-dioctylfluoren-2-ylethynyl)-N,N’-bis(2-ethylhexyl)-3,4,9,10-perylene diimide (**PDI1**). The crude product was purified by column chromatography (silica gel, chloroform). The product was obtained as a dark red solid (109 mg, 74% yield). ^{1}H NMR (400 MHz, CDCl$_3$): δ 10.22 (d, J = 8.3 Hz, 1H), 8.72 (s, 1H), 8.62 (d, J = 8.3 Hz, 1H), 8.58 (d, J = 8.0 Hz, 1H), 8.51 (d, J = 8.0 Hz, 1H), 8.44 (d, J = 8.2 Hz, 2H), 7.82-7.76 (m, 2H), 7.71 (s, 1H), 7.65 (dd, J_1 = 7.8 Hz, J_2 = 1.2 Hz, 1H), 7.46-7.37 (m, 3H), 4.29-4.03 (m, 4H), 2.23-2.04 (m, 4H), 2.03-1.86 (m, 2H), 1.51-1.27 (m, 16H), 1.23-1.06 (m, 20H), 0.97 (td, J_1 = 7.2 Hz, J_2 = 1.3 Hz, 6H), 0.91

(t, J = 7.0 Hz, 6H), 0.82-0.65 (m, 10H). ^{13}C NMR (126 MHz, $CDCl_3$): δ 163.70, 163.50, 163.47, 163.08, 151.50, 151.42, 143.20, 140.04, 138.45, 134.23, 134.05, 133.65, 133.13, 130.96, 130.89, 130.75, 130.64, 128.77, 128.18, 127.95, 127.10, 126.93, 126.60, 126.39, 126.33, 123.33, 123.21, 123.15, 123.09, 122.83, 122.76, 121.93, 120.49, 120.44, 120.23, 120.13, 102.30, 91.48, 55.42, 44.30, 40.33, 37.99, 31.79, 30.82, 30.07, 29.33, 29.29, 28.76, 24.11, 23.94, 23.14, 23.12, 22.61, 14.17, 14.08, 10.66, 10.64. HRMS (ESI) calcd. for $C_{71}H_{82}N_2O_4$ $[M+H]^+$ 1027.6353; found 1027.6350.

1-((7-(carbazol-9-yl)-9,9-dioctylfluoren-2-ylethynyl)-N,N'-bis(2-ethylhexyl)-3,4,9,10-perylene diimide (**PDI2**). The crude product was purified by column chromatography (silica gel, chloroform). The product was obtained as a black solid (172 mg, 70% yield).^{1}H NMR (400 MHz, $CDCl_3$): δ 10.05 (d, J = 8.3 Hz, 1H), 8.56 (s, 1H), 8.46 (dd, J_1 = 13.5 Hz, J_2 = 8.1 Hz, 2H), 8.33 (d, J = 8.0 Hz, 1H), 8.22 (dd, J_1 = 8.1 Hz, J_2 = 6.7 Hz, 2H), 8.15 (d, J = 7.8 Hz, 2H), 8.04 (d, J = 7.9 Hz, 1H), 7.91 (d, J = 7.8 Hz, 1H), 7.83 (s, 1H), 7.71 (dd, J_1 = 7.7 Hz, J_2 = 1.1 Hz, 1H), 7.68-7.63 (m, 2H), 7.50 (d, J = 8.2 Hz, 2H), 7.46-7.40 (m, 2H), 7.34-7.27 (m, 2H), 4.27-4.02 (m, 4H), 2.35-2.10 (m, 4H), 2.08-1.89 (m, 2H), 1.54-1.33 (m, 16H), 1.32-1.14 (m, 20H), 1.05-0.98 (m, 6H), 0.97-0.91 (m, 6H), 0.83-0.76 (m, 10H). ^{13}C NMR (126 MHz, $CDCl_3$): δ 163.54, 163.37, 163.29, 162.93, 153.37, 151.88, 142.31, 140.89, 139.22, 138.29, 137.45, 133.96, 133.83, 133.39, 132.97, 131.23, 130.68, 130.59, 130.50, 128.64, 127.86, 126.72, 126.56, 126.45, 126.10, 126.00, 123.49, 123.20, 123.14, 122.76, 122.67, 121.91, 121.89, 121.69, 120.58, 120.46, 120.43, 120.17, 120.06, 109.77, 102.20, 91.77, 55.82, 44.35, 44.32, 40.26, 38.02, 31.81, 30.86, 30.09, 29.43, 29.32, 28.78, 24.23, 24.14, 23.16, 23.14, 22.62, 14.19, 14.07, 10.66, 10.64. HRMS (ESI) calcd. for $C_{83}H_{89}N_3O_4$ $[M+H]^+$ 1192.6931; found 1192.6929.

1-(7-(anthracen-9-ylethynyl)-9,9-dioctylfluoren-2-ylethynyl)-N,N'-bis(2-ethylhexyl)-3,4,9,10-perylene diimide (**PDI3**). The crude product was purified by column chromatography (silica gel, chloroform). The product was obtained as a black solid (136 mg, 77% yield). ^{1}H NMR (400 MHz, $CDCl_3$): δ 10.18 (d, J = 8.3 Hz, 1H), 8.70 (s, 1H), 8.61 (t, J = 9.7 Hz, 3H), 8.52 (d, J = 8.0 Hz, 1H), 8.47 (d, J = 8.0 Hz, 1H), 8.40-8.31 (m, 3H), 7.94 (d, J = 8.4 Hz, 2H), 7.83 (s, 2H), 7.81-7.76 (m, 3H), 7.68 (d, J = 7.7 Hz, 1H), 7.60-7.53 (m, 2H), 7.50-7.43 (m, 2H), 4.27-4.06 (m, 4H), 2.32-2.18 (m, 4H), 2.10-1.90 (m, 2H), 1.53-1.31 (m, 16H), 1.30-1.11 (m, 20H), 1.00 (t, J = 7.3 Hz, 6H), 0.94 (t, J = 6.8 Hz, 6H), 0.90-0.81 (m, 4H), 0.76 (t, J = 6.5 Hz, 6H). ^{13}C NMR (126 MHz, $CDCl_3$): δ 206.97, 163.63, 163.45, 163.43, 163.05, 151.89, 151.78, 142.38, 140.49, 138.37, 134.06, 133.96, 133.47, 133.13, 132.48, 131.19, 131.14, 131.11, 130.77, 130.60, 128.66, 127.92, 127.72, 126.80, 126.68, 126.57, 126.52, 126.47, 126.15, 125.96, 125.65, 123.20, 123.18, 123.08, 123.04, 122.75, 122.66, 121.87, 120.78, 120.63, 120.18, 117.22, 102.07, 101.81, 91.95, 87.12, 55.71, 44.32, 40.38, 38.04, 31.82, 30.95, 30.87, 30.12, 29.42, 29.35, 28.80, 24.15, 24.10, 23.17, 23.14, 22.63, 14.19, 14.07, 10.68, 10.67. HRMS (ESI) calcd. for $C_{87}H_{90}N_2O_4$ $[M+H]^+$ 1227.6979; found 1227.7015.

2.3 Measurements

The NMR spectra were recorded in $CDCl_3$ on a Bruker Advance 400 MHz (for ^{1}H and ^{13}C NMR) or Bruker Advance 500 MHz (for ^{13}C NMR – target compounds) instruments.

Thermogravimetric analysis (TGA) was carried out on a Mettler Toledo TGA STARe system with a heating rate of 10 °C·min^{-1} in a constant stream of nitrogen (20 ml·min^{-1}). Differential Scanning Calorimetry (DSC) was performed with a Du Pont 1090B apparatus using a heating/cooling rate of 20 ºC·min^{-1} under nitrogen and aluminum sample pans. UV-Vis absorption spectra of solutions were recorded using an Evolution 220 UV-Visible Spectrophotometer at the concentration of 10^{-5} mol/L and 1 cm quartz cell and Jasco V-550 Spectrophotometer for films. Photoluminescence spectra of solutions were measured using Varian Carry Eclipse Spectrometer. Photoluminescence spectra in the solid state were monitored with Hitachi F-2500 Spectrometer. The quantum yield (Φ_f) measurements were performed by using the integrating sphere Avantes AvaSphere-80 (Edinburgh Instruments) and absolute method. The measurements were performed at room temperature with solvent (for liquid samples) or Spectralon® reflectance standard (for powdered samples) as blanks. Electrochemical measurements were carried out using Eco ChemieAutolab PGSTAT128n potentiostat, glassy carbon electrode (diam. 2 mm), platinum coil and silver wire as working, auxiliary and a reference electrode, respectively. Potentials are referenced with respect to ferrocene (Fc), which was used as the internal standard. Cyclic voltammetry experiments were conducted in a standard one-compartment cell, in CH_2Cl_2 (Carlo Erba, HPLC grade), under argon. 0.2 M Bu_4NPF_6 (Aldrich, 99%) was used as the supporting electrolyte. The concentration of compounds was equal $1.0\cdot10^{-6}$ mol/dm^3. Deaeration of the solution was achieved by argon bubbling through the solution for about 10 min before measurement. All electrochemical experiments were carried out under ambient conditions. Electroluminescence

(EL) spectra were measured with the voltage applied using a precise voltage supply (GwInstek PSP-405) and the sample was fixed to an XYZ stage. Light from the OLED device was collected through a 30 mm lens, focused on the entrance slit (50 μm) of a monochromator (Shamrock SR-303i) and detected using a CCD detector (Andor iDus 12305). Typical acquisition times were equal to 10 seconds. The pre-alignment of the setup was done using a 405 nm laser. The layers' thickness were measured using an AFM Park XE-100 instrument (Park System, Korea) operating in tapping mode in the air with standard 125 μm single-crystal silicon cantilevers. The piezoelectric scanner had a scan range of approximately 100 μm x 100 μm.

2.4 Film preparation

Films on glass substrates were prepared from a homogeneous chloroform solution (10 mg/ml) by spin-coating method (1000 rpm, 60 s). Films were dried for 24h in a vacuum oven at 50 °C.

2.5 Device preparation

Devices with sandwich configuration ITO/PEDOT:PSS/**PDI**/Al were prepared on OSSILA substrates with pixilated ITO anodes, cleaned with detergent, deionized water, 10% NaOH solution, water, and isopropyl alcohol in an ultrasonic bath. Substrates were covered with PEDOT:PSS film by spin-coating at 5000 rpm for 60 s and annealed for 5 min at 120 °C. The active layer was spin-coated on top of the PEDOT:PSS layer from a chloroform solution (10 mg/mL) at 1000 rpm for 60 s and annealed for 5 min at 100 °C. Finally, Al was vacuum-deposited at a pressure of $5\cdot 10^{-5}$ Torr.

2.6 DFT calculation

The calculations were carried out using Gaussian09 [31] program. Molecular geometries of the singlet ground state of the compounds were optimized in the gas phase at the B3LYP/6-31g^{++} level of theory. For each compound a frequency calculation was carried out, verifying that the obtained optimized molecular structure corresponds to an energy minimum, thus only positive frequencies were expected. The contribution of a group (anthracene and carbazole) to a molecular orbital was calculated using Mülliken population analysis. GaussSum 3.0

program [32] was used to calculate group contributions to the molecular orbitals and to prepare the partial density of states (DOS) spectra.

3. Result and discussion

3.1 Synthesis

The synthetic routes of intermediates and target compounds are shown in Schemes 1 and 2. The key intermediates **1-13** and ethynyl derivatives (**Et-1 – Et-3)** were synthesized according to the well-known procedures with minor modifications [33-41]. Briefly, the iodination of fluorene gave 2-iodofluorene **1** and 2,7-diiodofluorene **4** which reacted with *n*-octyl bromide in the presence of tetra-*n*-butyl ammonium bromide (TBAB) as phase transfer catalysis (PTC) formed 2-iodo-9,9-dioctylfluorene **2** and 2,7-diiodo-9,9-dioctylfluorene **5** with high yield. The Ullmann condensation of carbazole with **5** in the presence of CuI/1,10-phenanthroline as catalysts produced **6** in 59% yield. Next, a Sonogashira cross-coupling reaction of trimethylsilylacetylene (TMSA) with **2** and **6** in the presence of $[Pd(PPh_3)_4]$/CuI as catalysts afforded **3** and **7**. Treatment with NaOH converted compounds **3** and **7** into 2-ethynyl-9,9-dioctylfluorene (**Et-1**) and 2-ethynyl-7-(carbazol-9-yl)-9,9-dioctylfluorene (**Et-2**).

Compound **Et-3** was obtained in a four-step reaction. First, the bromination of fluorene gave **8** with 86% yield. Then, N-alkylation of **8** provided 2,7-dibromo-9,9-dioctylfluorene (**9**). Sonogashira cross-coupling reaction of deficiency of TMSA with **9** afforded **10** which was converted to 1-(7-ethynyl-9,9-dioctylfluoren-2-yl)ethynylanthracene (**Et-3**) (73% yield) by treatment with NaOH. A brominated derivative of perylene bisimide **13** was obtained by imidization reaction between 3,4,9,10-perylenetetracarboxylic dianhydride and 2-ethylhexylamine to give perylene bisimide **12** in 83% yield, then **12** was converted to key intermediate **13** by a selective bromination reaction using bromine. The desired perylene bisimide derivatives (**PDI1–PDI3**) were prepared by Pd-catalyzed Sonogashira cross-coupling reaction of the respective ethynyl derivatives **Et-1**, **Et-2** or **Et-3** with **13** (Scheme 2). The obtained compounds **PDI1–PDI3** were fully characterized by standard spectroscopic methods (^{1}H and ^{13}C NMR, mass spectrometry). The final compounds **PDI1–PDI3** exhibit excellent solubility in common organic solvents, such as hexane, dichloromethane, chloroform, toluene, and tetrahydrofuran.

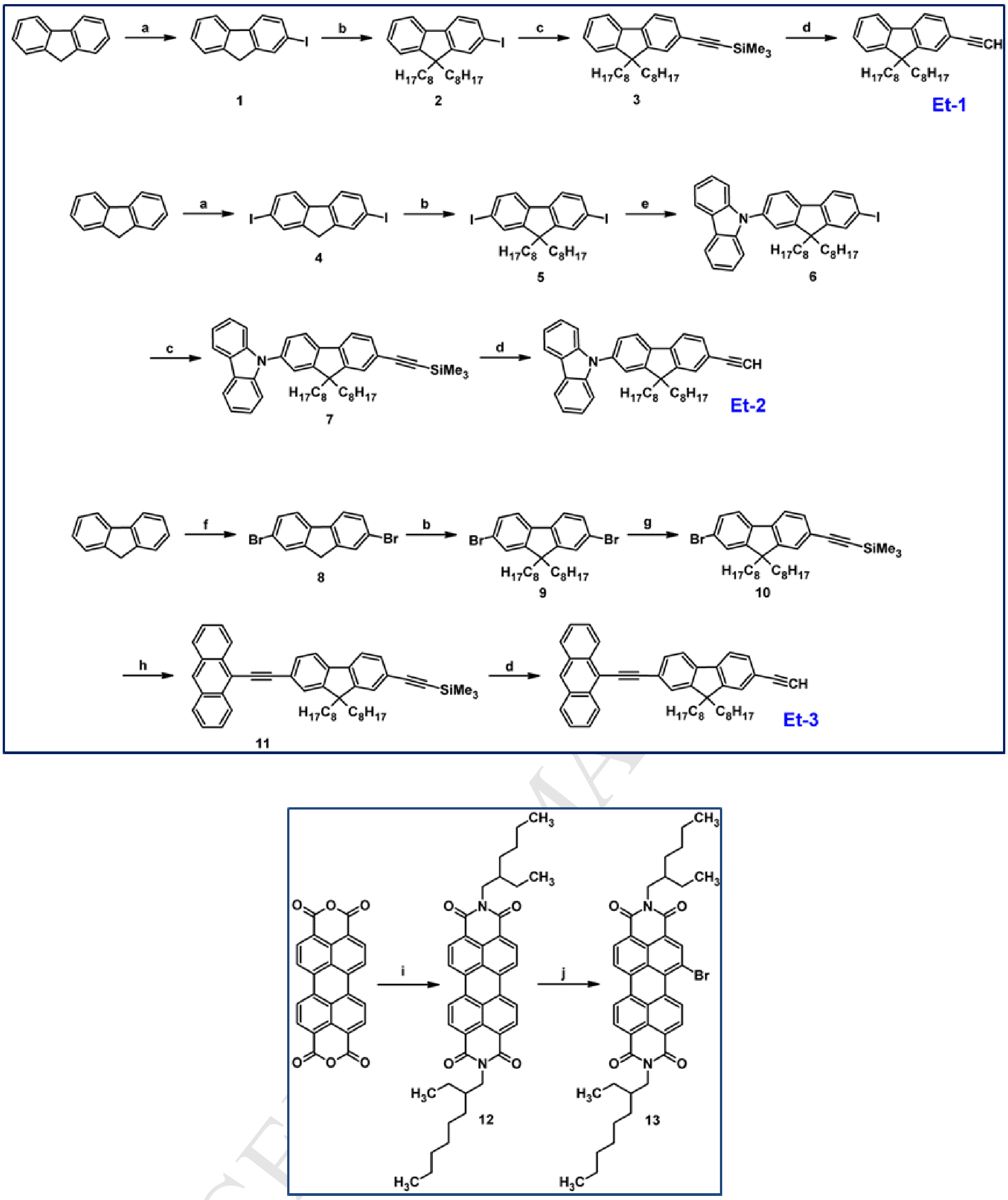

Scheme 1. Synthesis of compounds **1-13**. *Reagents and conditions:* **(a)** I_2, H_5IO_6, $AcOH/H_2O/H_2SO_4$, 70 °C, 6h; **(b)** 50% NaOH, TBAB, *n*-$C_8H_{17}Br$, DMSO, room temp., 12h; **(c)** TMSA, $Pd(PPh_3)_4$, CuI, TEA, room temp., 24h; **(d)** NaOH, MeOH/THF, room temp., 6h; **(e)** carbazole, CuI, K_2CO_3, 1,10-phenanthroline, DMF, reflux, 30h; **(f)** Br_2, Fe, $CHCl_3$, 0 °C, 4h; **(g)** TMSA, $Pd(PPh_3)_4$, CuI, TEA/PhMe, 35 °C, 20h; **(h)** 9-ethynylanthracene, $Pd(PPh_3)_4$, CuI, TEA, 80 °C, 30h; **(i)** 2-ethylhexylamine, DMF, reflux, 8h; **(j)** Br_2, DCM, room temp., 72h.

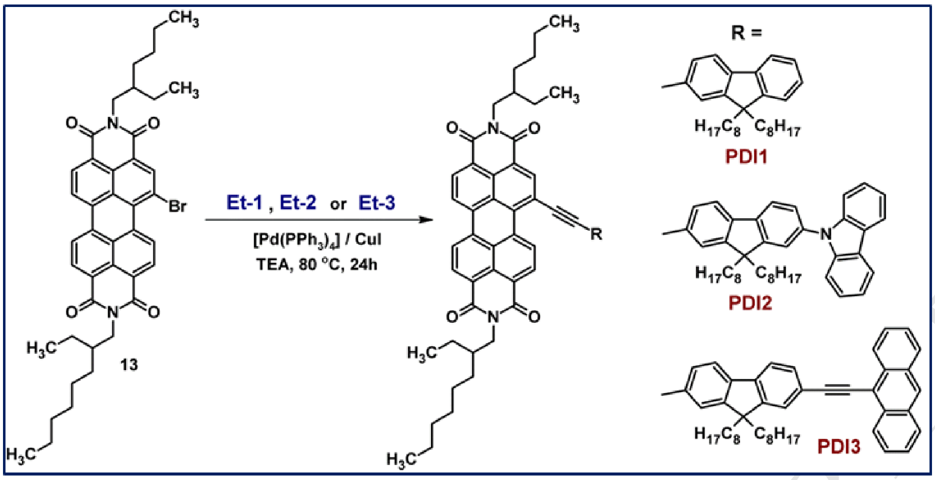

Scheme 2. The synthetic route for the preparation of compounds **PDI1–PDI3**.

3.2 DSC and TGA studies

The thermal properties of luminescent materials are important for achieving high performance and long-lifetime optoelectronic devices [42] Thermal properties of the synthesized unsymmetrical bay substituted acetylene perylene diimides **PDI1–PDI3** were evaluated by differential scanning calorimetry (DSC) and thermogravimetric analysis (TGA) carried out under a nitrogen atmosphere. The obtained data are summarized in Table 1.

Table 1. The thermal properties of synthesized perylene diimide derivatives **PDI1–PDI3**.

Code	DSC	TGA		
	T_g [°C]	T_5 [°C]	T_{10} [°C]	Residue at 800°C [%]
PDI1	135	369	419	33
PDI2	130	419	440	10
PDI3	98	425	443	21

All compounds gave similar DSC profiles with glass transition temperature (T_g) registered at 135, 130 and 98 °C for **PDI1**, **PDI2**, and **PDI3**, respectively (Fig. S1). It was observed that the presence of second acetylene unit in **PDI3** lowered the T_g value. The measurements confirmed that the derivatives are amorphous materials and no peaks due to crystallization and melting appeared in DSC thermograms. TGA thermograms showed that for the obtained compounds, thermal decomposition started when detected as 5% weight loss (T_5) above 369 °C. Based on T_5 and the temperature of 10% weight loss (T_{10}) it can be concluded that the introduction of carbazole (**PDI2**) and anthracene unit (**PDI3**) improves the thermal stability of perylene diimide derivatives.

3.3 UV-Vis absorption and emission investigations

Absorption and emission properties of the prepared perylene diimides **PDI1–PDI3** were studied by means of UV-Vis and photoluminescence (PL) spectroscopy in chloroform solution and in the solid state as thin film on glass substrates. Electroluminescence ability of the obtained molecular glasses was studied for diodes of the following configuration: ITO/PEDOT:PSS/**compound**/Al. UV-Vis absorption spectra of investigated compounds both in chloroform solution and as thin film were depicted in Fig. 1, whereas the spectroscopic data are summarized in Table 2.

(a)

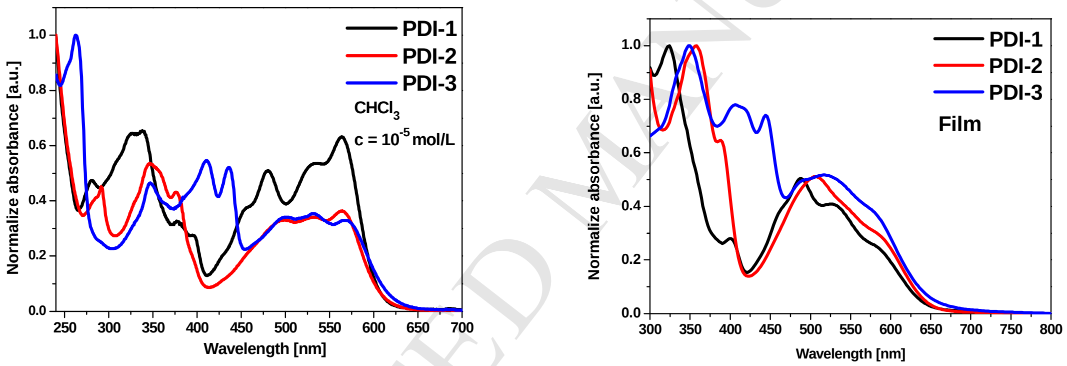

(b)

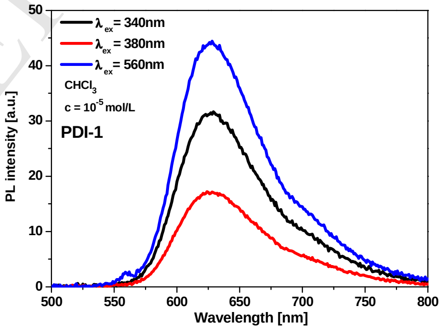

(c)

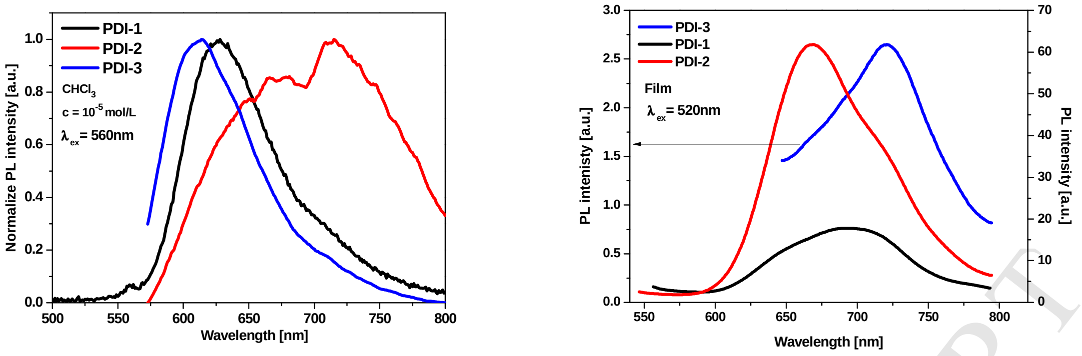

Fig. 1. (a) Normalized absorption spectra of **PDI1–PDI3** in chloroform solution and films; (b) photoluminescence spectra of **PDI1** in solution under various λ_{ex} and (c) PL spectra of **PDI1–PDI3** in chloroform solution and films.

Table 2. UV-Vis, photoluminescence and electroluminescence data of bay substituted perylene diimides **PDI1–PDI3**.

Code	UV-Vis λ_{max} [nm] ($\varepsilon \cdot 10^4$)^a		PL λ_{em} [nm] (Stokes shift [cm^{-1}])		(Φ_{PL}) [%]		EL λ_{EL}[nm]
	CHCl$_3$^{b}	Film	CHCl$_3$^{b}	Film	CHCl$_3$^{b}	Film	
PDI1	278(1.3); 338 (1.8); 377 (0.9); 448 (1.3); 479 (1.4); 529 (2.1); 563 (1.8)	324; 400; 488; 526; 583^{sh}	621 (1658)	691 (4540)	79	28	706
PDI2	291 (2.5); 344 (3.0); 376 (2.4); 497 (1.8); 532 (1.9); 563 (2.0)	358;388; 506; 591^{sh}	661(2633); 711(3697)	668 (4792)	15	20	685
PDI3	261 (2.9); 347 (1.8); 410 (2.1); 436 (2.0); 495 (0.9); 526 (0.9); 561 (0.9)	349;406; 444; 522;580^{sh}	613 (1512)	720 (5269)	17	19	732
^{a}molecular absorption coefficient [dm^3· mol^{-1}· cm^{-1}]; ^{b}c=10^{-5}mol/L							

Typically PDI-based molecules exhibited strong absorption in the range of 400-550 nm with two sharp maxima (λ_{max}) at about 480 and 520 nm corresponding to 0-0 and 0-1 vibrational transition of perylene diimide unit [43,44]. In the case of investigated compounds except absorption characteristic for perylene diimide structure also band at higher energy in the range of 300-400 nm due to the presence of fluorene derivative was seen. Compound bearing anthracene moiety (**PDI3**) exhibited additionally absorption band with a pronounced vibrational structure with λ_{max} at 410 and 436 nm. The absorption band at a higher energy range of the compounds in films is slightly bathochromic shifted compared to its in solution, indicating the weak aggregation in the solid state (Fig. S2).

The effect of the excitation wavelength (λ_{ex}) on maximum emission band (λ_{em}) and its intensity was evaluated and representative PL spectra of **PDI1** obtained under various λ_{ex} are shown in Fig. 1b. The utilization of λ_{ex} = 560 nm resulted in the highest PL intensity. All studied perylene diimides were photoluminescent both in solution and in the solid state and emitted red radiation with PL quantum yield in the range of 15-79 % in solution and 19-28 % in film, respectively. Compounds **PDI1–PDI3** in the solid state exhibited large Stokes shifts ranging above 4540 cm^{-1}. Organic emitting compounds with large Stokes' shift are desired for various application including lighting and photovoltaic technologies [45]. The presence of an additional substituent at the fluorene unit (**PDI2** and **PDI3**) influences on the emission spectra. It was found that substitution of fluorene with N-carbazole moiety (**PDI2**) significantly reduced emission intensity and shifted λ_{em} to lower energy in solution. On the other hand, **PDI2** in film emitted light with the highest intensity. The presence of second acetylene bond together with anthracene unit (**PDI3**) in film lowered PL intensity. However, the relationship between structure and PL intensity does not correspond to EL intensity. Considering the EL spectra depicted in Fig. 2 compound without substituted fluorene unit (**PDI1**) showed the lowest intensity of emitted light under external voltage, which was the most intense in the case of molecule bearing anthracene structure (**PDI3**).

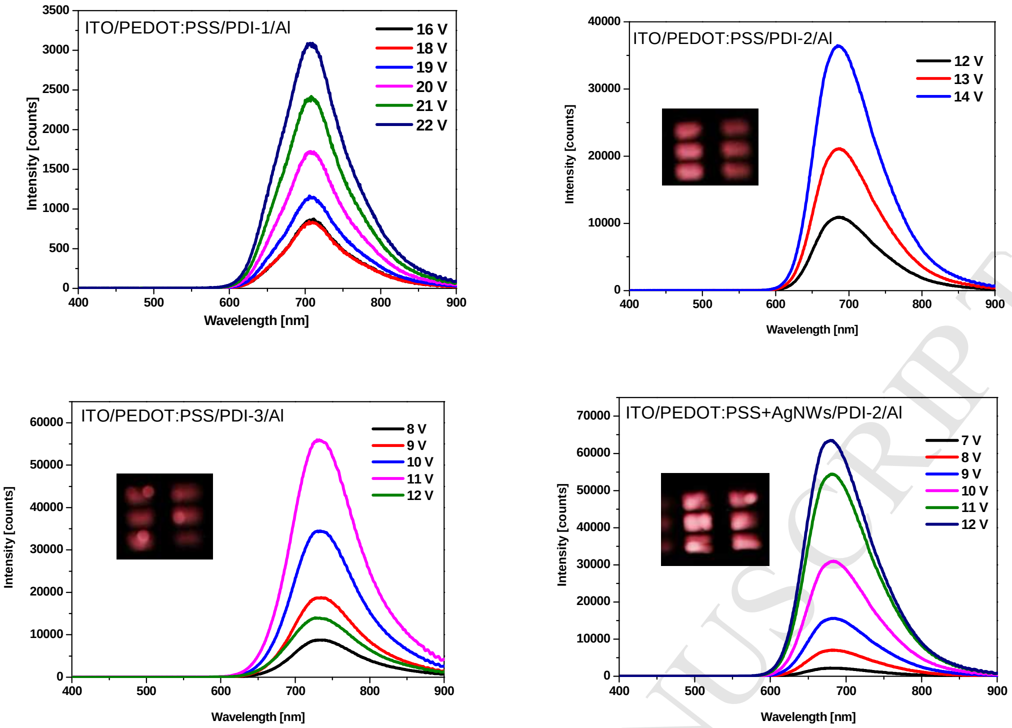

Fig. 2. Electroluminescence spectra of fabricated diodes as a function of the applied voltage.

All the devices based on the PDI derivatives showed electroluminescence and emitted light with a maximum of EL band ranging from 685 to 732 nm (Table 2). In the case of devices based on **PDI1** and **PDI2** together with the increase of applied voltage the increase of intensity of emitted light was observed contrary to the diode with **PDI3** (Fig. S3). For diode contains **PDI3** the intense of electroluminescence rapidly decreases above external voltage above 11 V. Device based on **PDI3** exhibited the best performance considering the EL intensity. Additionally, in order to test the possibility of the EL intensity enhancing in OLED devices a layer of silver nanowires (AgNWs) was incorporated during the preparation of the diode based on **PDI2**. Device with structure ITO/PEDOT:PSS/AgNWs(1:1)/**PDI2**/Al was prepared. Considering the EL spectra of such diode depicted in Fig. 2, when **PDI2** mixed with plasmonically active silver nanowires, the compounds exhibited significantly stronger electroluminescence signal, associated presumably with plasmonics enhancement [46,47].

3.4 Quantum calculations

To gain further insight into the electronic structure of the compounds the quantum theoretical calculations at the density functional theory level were performed. Based on the optimized geometries the energy and electronic distribution of molecular frontier orbitals were calculated in dichloromethane for a comparison with experimental (electrochemical) potentials. Three-dimensional plots of the electron density for the highest occupied molecular orbital (HOMO) and the lowest unoccupied molecular orbital (LUMO) of **PDI1–PDI3** are shown in Fig. 3, whereas the orbital energies and compositions are summarized in Table S1 in SI.

LUMO **HOMO**

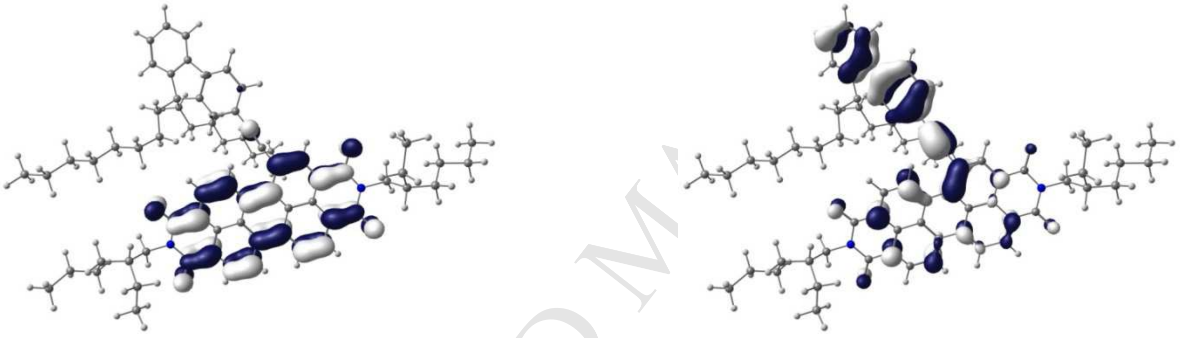

PDI1

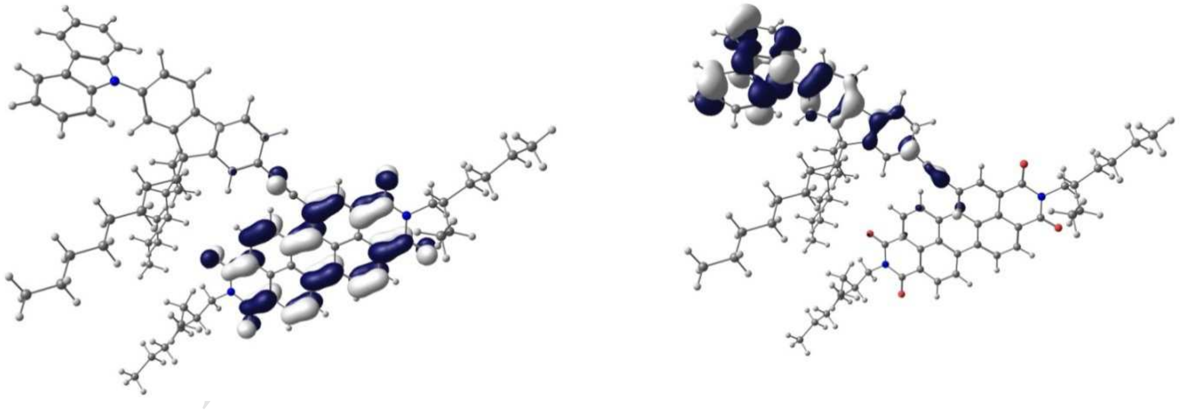

PDI2

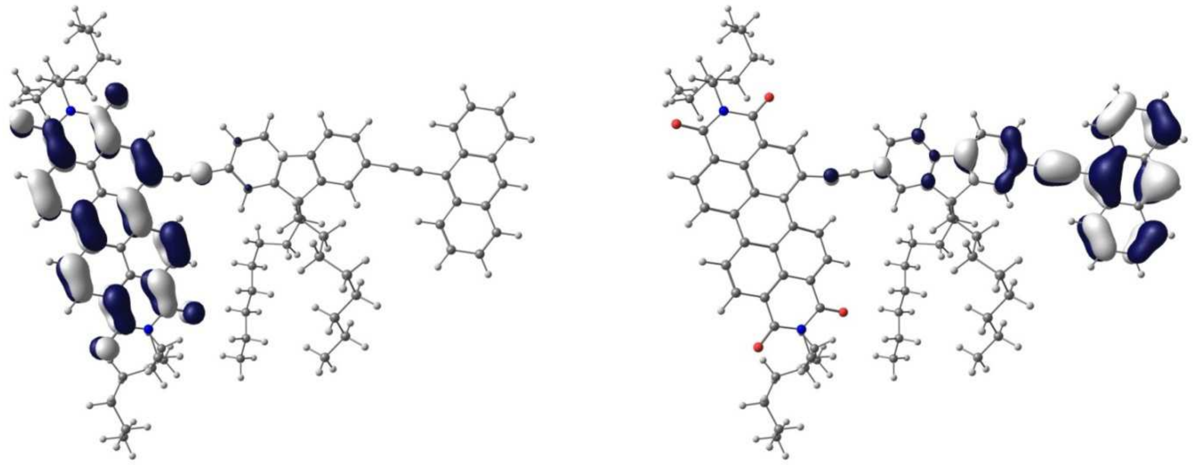

PDI3

Fig. 3. Contours of HOMOs and LUMOs of **PDI1–PDI3** compounds.

Moreover, Fig. S4 in Supplementary Materials shows the partial density of states diagrams. The molecule of each compound was divided into two fragments such as perylene diimide, 2-etynylfluorene (R) with appropriate alkyl chains and the substituent (R') in fluorene moiety, respectively and their contribution to each molecular orbital was calculated. The electronic structures of the compounds of **PDI2–PDI3** are similar and HOMOs are localized on the substituent (R and R') in the perylene moiety (Fig. 3, Fig. S4, and Table S1). In the case of **PDI1** both molecule aromatic fragments i.e. perylene diimide and 2-etynylfluorene participate in HOMO. LUMOs in each case are localized on the antibonding orbitals of perylene diimide moiety. The calculated energies of LUMO are the same for each molecule which is understandable considering the electronic structures of these compounds. HOMO energies increase in the range of **PDI1** to **PDI3**. The increase of the HOMO energy is related to the molecular structure of the **R** and **R'** substituents and thus its effect on the electronic structure of the molecule. So, in the **PDI2** and **PDI3** molecules the LUMO is mainly localized on the **R'** substituent in the fluorene part i.e. carbazole and ethynyl anthracene moieties, respectively (Table S1).

3.5 Electrochemical properties

The electrochemical properties of **PDI1–PDI3** were investigated in CH_2Cl_2 solution by means of cyclic voltammetry (CV). The electrochemical oxidation and reduction onset potentials were used for estimation of the HOMO and LUMO energies (or rather, ionization potentials and electron affinities) of the materials (assuming that IP of ferrocene equals -5.1 eV) [48]. The calculated HOMO and LUMO levels together with electrochemical energy band gap (Eg) are presented in Table 3. All measurements were carried out on glassy carbon electrode (the working electrode). In comparison to the platinum electrode, it allows to record up to three separate reduction peaks (for **PDI3**), which was not possible on platinum wire (diam. 1mm) electrode.

Table 3. The calculated HOMO and LUMO levels together with electrochemical energy band gap (Eg).

Code	E_{1red} [V]	E_{2red} [V]	E_{3red} [V]	E_{1ox} [V]	E_{2ox} [V]	HOMO[a] (CV)	LUMO[b] (CV)	HOMO (DFT)	LUMO (DFT)	$E_{g(CV)}$[c] [eV]	$E_{g(DFT)}$ [eV]
PDI1	-1.02	-1.15	-	0.96	1.10	-6.06	-4.08	-5.66	-3.54	1.98	2.12
PDI2	-0.99	-1.10	-	0.74	1.05	-5.84	-4.11	-5.43	-3.54	1.73	1.89
PDI3	-0.97	-1.08	-2.01	0.59	-	-5.69	-4.13	-5.18	-3.53	1.56	1.65

[a]HOMO= -5.1- E_{ox};[b]LUMO= -5.1-E_{red}[c]E_g= E_{ox} (onset) −E_{red}(onset)

For each polyimide a fully reversible reduction process towards the formation of an anion radical according to mechanism put forward by S.-H. Hsiao et al. [49] was recorded (similar as we reported before [50,51]).

The first reduction peak onset (E_{1red}) is as high as -1.02, -0.99, and -0.97 V for **PDI1**, **PDI2**, and **PDI3**, respectively (Fig. S5). This process is ascribed to the reduction of the imide core (i.e. PDI/PDI$^-$). However, the values in each case are significantly lower compared with the unsubstituted perylene derivatives [52]. This is a direct consequence of π-excessing moieties incorporation in PDI's position 1, proving a strong influence on physical properties. By further lowering of potential all imides underwent second reduction step (PDI$^-$/PDI^{2-}), also fully reversible. It is worth noting that difference of ending group in the molecule chain in each case affected reduction values, but not change the high stability of PDI anion and dianion itself. Finally, for **PDI3** the third reduction peak at a potential slightly below -2 V was also recorded. In this potential region, only this molecule underwent the reduction process, which suggests, that it is the reduction of anthracene moiety (Fig. 4).

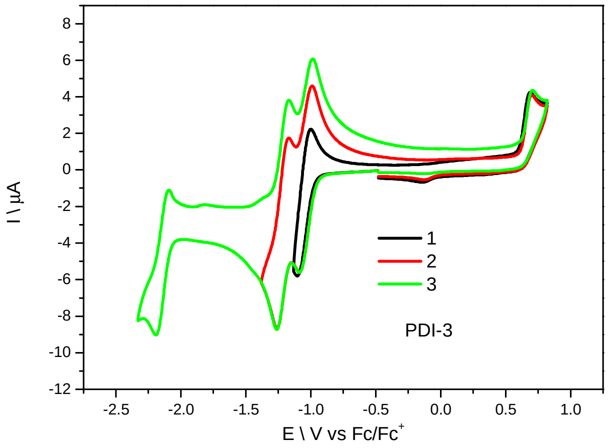

Fig. 4. Cyclic voltammograms for **PDI3**. CV sweep ratev = 100 mV/s, 0.1 M Bu_4NPF_6 in CH_2Cl_2 with different lower vertex potential.

On the other hand, for **PDI1** and **PDI3** oxidation was non-reversible (E_rC_i type, which means that reversible electrochemical reaction (E_r) is followed by an irreversible chemical reaction (C_i)), with onsets at 0.96 and 0.52 V, respectively. In the case of **PDI2** oxidation is slightly different in nature, giving characteristic carbazole/carbazole$^+$ response. Taking into consideration this fact, the possibility of anodic polymerization was evaluated. As can be seen in Fig. 5 after first cycle new peak with onset at 0.46 appears.

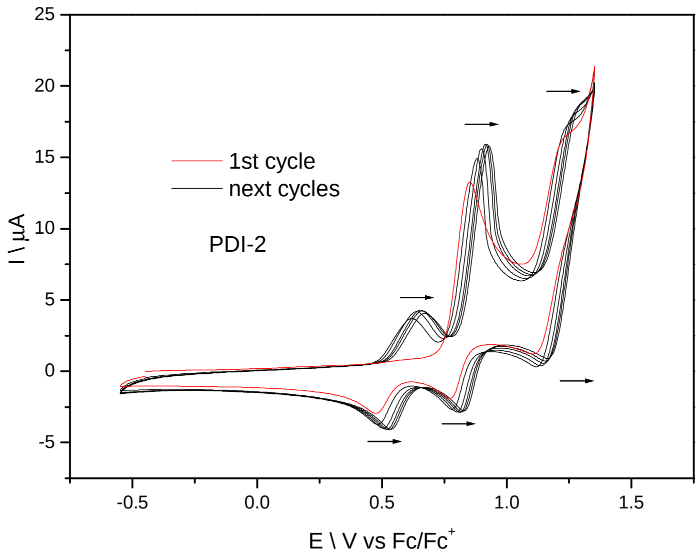

Fig. 5. Cyclic voltammograms for **PDI2**. CV sweep rate ν = 100 mV/s, 0.1 M Bu_4NPF_6 in CH_2Cl_2. Arrows indicate shifts in peak maxima.

Nevertheless, electrochemically determined band gaps for the investigated PDIs are as follow 1.97, 1.73, and 1.57 eV. For **PDI1** this value is in agreement with optical band gap (2.02 eV) while in the case of **PDI3** difference is quite high, suggesting that HOMO and LUMO are separated in space. The electrochemical study shows that introduction into PDI molecule a moiety with the desired redox properties can modify the electrochemical properties of the final material. Very good reduction properties of the studied compounds, make them good candidates for new organic n-type semiconductors, which is extremely important for the organic electronics field.

4. Conclusion

The synthesis and characterization of novel perylene diimides with bulky aromatic moieties in bay positions were reported. The introduction of aromatic substituents to perylene core as well as N-substitution by 2-ethylhexyl group considerably improves solubility and prevents aggregation and π-πstacking of PDIs. The presence of substituents in bay positions of PDIs has an impact on their properties. The prepared perylene diimides were amorphous and showed T_g ranging from 98 to 135 ºC. The presence of carbazole structure (**PDI2**) resulted in an increase of T_g. They exhibited high thermal stability with the beginning of decomposition above 370 ºC. All examined perylene diimides are photo- and electroluminescent. They emitted light in the deep red region. The substitution of fluorene in diimide with carbazole and anthracene units significantly reduced PL intensity in solution, however, had a less pronounced impact on PL quantum yield in the solid state. The introduction of carbazole derivative into PDI hypsochromically shifted, compared to the others, the maximum of PL and EL bands. It was found that compound bearing anthracene unit (**PDI3**) exhibited the most intense electroluminescence under the lowest applied voltage. Thus, it seems to be the most promising for further investigations.

Acknowledgment

This work was supported by the National Science Centre of Poland, Projects OPUS-11 No 2016/21/B/ST5/00805 and Sonata Bis DEC-2013/10/E/ST3/00034. Calculations were carried out at the Wroclaw Centre for Networking and Supercomputing (http:// www.wcss.wroc.pl); grant number No.18. We particularly indebted to Dr. Henryk Janeczek for DSC measurements.

References

[1] Yan Q, Zhao D. Conjugated dimeric and trimeric perylenediimide oligomers. Org Lett 2009;11:3426–3429.

[2] Reghu RR, Bisoyi HK, Grazulevicius JV, Anjukandi P, Gaidelis V, Jankauskas V. Air stable electron-transporting and ambipolar bay substituted perylene bisimides. J Mater Chem 2011;21:7811-7819.

[3] Mumyatov AV, Leshanskaya LI, Anokhin DV, Dremova NN, Troshin PA. Organic field-effect transistors based on disubstituted perylene diimides: Effect of alkyl chains on the device performance. Mendeleev Commun 2014;24:306-307.

[4] Liu J, Zheng N, Hu Z, Wang Z, Yang X, Huang F, Cao Y. Self-doped n-type small molecular electron transport materials for high-performance organic solar cells. Sci China Chem 2017;60:1136-1144.

[5] Yang Y, Wang Y, Xie Y, Xiong T, Yuan Z, Zhang Y, Qian S, Xiao Y. Fused perylenebisimide-carbazole: new ladder chromophores with enhanced third-order nonlinear optical activities. Chem Commun 2011;47:10749-10751.

[6] Yi J, Wang J, Lin Y, Gao W, Ma Y, Tan H, Wang H, Ma C-Q. Molecular geometry regulation of bay-phenyl substituted perylenediimide derivatives with bulky alkyl chain for use in organic solar cells as the electron acceptor. Dyes Pigments 2017;136:335-346.

[7] Yi M, Yi J, Wang J, Wang L, Gao W, Lin Y, Luo Q, Tan H, Ma Ch-Q, Wang H. Perylenediimide derivatives based on a dendritic oligothiophene core as electron acceptor for use in polymer solar cells. Dyes Pigments 2017;139:498-508.

[8] Li G, Zhao Y, Li J, Cao J, Zhu J, Sun XW, Zhang Q. Synthesis, Characterization, Physical Properties, and OLED Application of Single BN-Fused Perylene Diimide. J Org Chem 2015;80:196-203.

[9] Wei Q, Wang W, Zhou E, Liu X-P, Liang M-H, Deng K, Yang J-K, Jiang P. Positioned substituent effect on self-assembly behaviors of perylene diimide derivatives on graphite. J Colloid Interface Sci 2017;504:58-67.

[10] Dhokale B, Jadhav T, Patil Y, Misra R. Symmetrical and unsymmetrical ferrocenyl perylenediimides: Design, synthesis and properties. Dyes Pigments 2016;134: 164-170.

[11] Lucenti E, Botta C, Cariati E, Righetto S, Scarpellini M, Tordin E, Ugo R. New organic-inorganic hybrid materials based on perylene diimide-polyhedral oligomeric

silsesquioxane dyes with reduced quenching of the emission in the solid state. Dyes Pigments 2013;96:748-755.

[12] Adhikari T, Rahami ZG, Nunzi JM, Lebel O. Synthesis, characterization and photovoltaic performance of novel glass-forming perylenediimide derivatives. Org Electron 2016;34:146-156.

[13] Koch M, Myahkostupov M, Oblinsky DG, Wang S, Garakyaraghi S, Castellano FN, Scholes GD. Charge Localization after Ultrafast Photoexcitation of a Rigid Perylene Perylenediimide Dyad Visualized by Transient Stark Effect. J Am Chem Soc 2017;139:5530-5537.

[14] Singh TB, Erten S, Gunes S, Zafer C, Turkmen G, Kuban B, Teoman Y, Sariciftci NS, Icli S. Soluble derivatives of perylene and naphthalene diimide for n-channel organic field-effect transistors. Org Electron 2006;7:480-489.

[15] Chen Z, Stepanenko V, Dehm V, Prins P, Siebbeles LDA, Seibt J, Marquetand P, Engel V, Wurthner F. Photoluminescence and conductivity of self-assembled π-π stacks of perylene bisimide dyes. Chem A Eur J 2007;13:436-449.

[16] Van Herrikhuyzen J, Syamakumari A, Schenning APHJ, Meijer EW. Synthesis of n-type perylene bisimide derivatives and their orthogonal self-assembly with p-type oligo(p-phenylene vinylene)s. J Am Chem Soc 2004;126:10021-10027.

[17] Langhals H, Ismael R, Yuruk O. Persistent Fluorescence of Perylene Dyes by Steric Inhibition of Aggregation. Tetrahedron 2000;56:5435-5441.

[18] Langhals H, Krotz O, Polborn K, Mayer P. A Novel Fluorescent Dye with Strong, Anisotropic Solid-State Fluorescence, Small Stokes Shift, and High Photostability. Angew Chem Int Ed 2005;44:2427-2428.

[19] Huang C, Barlow S, Marder SR. Perylene-3,4,9,10-tetracarboxylic acid diimides: synthesis, physical properties, and use in organic electronics. J Org Chem 2011;76:2386-2407.

[20] Kozma E, Mroz W, Villafiorita-Monteleone F, Galeotti F, Andicsova-Eckstein A, Catellania M, Botta C. Perylene diimide derivatives as red and deep red emitters for fully solution processable OLEDs. RSC Adv 2016;6:61175-61179.

[21] Li G, Zhao Y, Li J, Cao J, Zhu J, Sun XW, Zhang Q. Synthesis, Characterization, Physical Properties, and OLED Application of Single BN-Fused Perylene Diimide. J Org Chem 2015;80:196-203.

[22] Pan J, Zhu W, Li S, Zeng W, Cao Y, Tian H. Dendron-functionalized perylene diimides with carrier-transporting ability for red luminescent materials. Polymer 2005;46:7658-7669.

[23] Chen K-Y, Chow TJ. 1,7-Dinitroperylene bisimides: facile synthesis and characterization as n-type organic semiconductors. Tetrahedron Lett 2010;51:5959-5963.

[24] Zhang Z, Lei T, Yan Q, Pei J, Zhao D. Electron-transporting PAHs with dual perylenediimides: synthesis and semiconductive characterizations. Chem Commun 2013;49:2882-2884.

[25] Chang H, Chen Z, Yang X, Yin Q, Zhang J, Ying L, Jiang X-F, Xu B, Huang F, Cao Y. Novel perylene diimide based polymeric electron-acceptors containing ethynyl as the π-bridge for all-polymer solar cells. Org Electron 2017;45:227-233.

[26] Xiong W, Meng X, Liu T, Cai Y, Xue X, Li Z, Sun X, Huo L, Ma W, Sun Y. Rational design of perylenediimide-based polymer acceptor for efficient all-polymer solar cells. Org Electron 2017;50:376-383.

[27] Kozma E, Kotowski D, Catellani M, Luzzati S, Famulari A, Bertini F. Synthesis and characterization of new electron acceptor perylenu diimide molecules for photovoltaic applications. Dyes Pigments 2013;99:329-338.

[28] Ford WE, Kamat PV. Photochemistry of 3,4,9,10-perylenetetracarboxylic dianhydride dyes. 3. Singlet and triplet excited-state properties of the bis(2,5-di-tert-butylphenyl)imide derivative. J Phys Chem 1987;91:6373-6380.

[29] Suganya S, Namgoong JW, Mutyala AK, Velmathi S, Kim JP, Park JS. A new perylenediimide with NH functionality as a colorimetric and fluorescent probe for the selective detection of trivalent Fe^{3+} and Al^{3+} ions. J Photochem Photobiol A: Chemistry 2017;344:36-41.

[30] Belfield KD, Bondar MV, Hernandez FE, Przhonska FEJ. Photophysical Characterization, Two-Photon Absorption and Optical Power Limiting of Two Fluorenylperylene Diimides. J Phys Chem C 2008;112:5618-5622.

[31] Frisch M. J, Trucks G. W, Schlegel H. B, Scuseria G. E, Robb M. A, Cheeseman J. R, Scalmani G, Barone V, Mennucci B, Petersson G. A, Nakatsuji H, Caricato M, Li X, Hratchian H. P, Izmaylov A. F, Bloino J, Zheng G, Sonnenberg J. L, Hada M, Ehara M, Toyota K, Fukuda R, Hasegawa J, Ishida M, Nakajima T, Honda Y, Kitao O, Nakai H, Vreven T, Montgomery, Jr. J. A, Peralta J. E, Ogliaro F, Bearpark M, Heyd

J. J, Brothers E, Kudin K. N, Staroverov V. N, Kobayashi R, Normand J, Raghavachari K, Rendell A, Burant J. C, Iyengar S. S, Tomasi J, Cossi M, Rega N, Millam J. M, Klene M, Knox J. E, Cross J. B, Bakken V, Adamo C, Jaramillo J, Gomperts R, Stratmann R. E, Yazyev O, Austin A. J, Cammi R, Pomelli C, Ochterski J. W, Martin R. L, Morokuma K, Zakrzewski V. G, Voth G. A, Salvador P, Dannenberg J. J, Dapprich S, Daniels A. D, Farkas O, Foresman J. B, Ortiz J. V, Cioslowski J, Fox D. J (2009) Gaussian, Inc., Gaussian 09, Revision A.1, Wallingford CT.

[32] O'Boyle NM, Tenderholt AL, Langner KM. J Comp Chem 2008;29:839-845.

[33] Lee SH, Nakamura T, Tsutsui T. Synthesis and Characterization of Oligo(9,9-dihexyl-2,7-fluorene ethynylene)s: For Application as Blue Light-Emitting Diode. Org Lett 2001;3:2005-2007.

[34] Ma X, Jiao J, Yang J, Huang X, Cheng Y, Zhu C. Large stokes shift chiral polymers containing (R,R)-salen-based binuclear boron complex: Synthesis, characterization, and fluorescence properties. Polymer 2012;53:3894-3899.

[35] Ma X, Azeem EA, Liu X, Cheng Y, Zhu C. Synthesis and tunable chiroptical properties of chiral BODIPY-based D–π–A conjugated polymers. J Mater Chem. C 2014;2:1076-1084.

[36] Khan MS, Al-Mandhary MRA, Al-Suti MK, Ahrens B, Mahon MF, Male L, Raithby PR, Boothby CE, Köhler A. Synthesis, characterisation and optical spectroscopy of diynes and poly-ynes containing derivatised fluorenes in the backbone. Dalton Trans 2003:74-84.

[37] Lin Y, Chen Y, Ye T-L, Chen Z-K, Dai Y-F, Ma D-G. Oligofluorene-based push–pull type functional materials for blue light-emitting diodes. J Photochem Photobiol A: Chemistry, 2012;230:55-64.

[38] Yang J, Jiang C, Zhang Y, Yang R, Yang W, Hou Q, Cao Y. High-Efficiency Saturated Red Emitting Polymers Derived from Fluorene and Naphthoselenadiazole. Macromolecules 2004;37:1211-1218.

[39] Islam SN, Sil A, Patra SK. Achieving yellow emission by varying the donor/acceptor units in rod-shaped fluorenyl-alkynyl based π-conjugated oligomers and their binuclear gold(I) alkynyl complexes. Dalton Trans 2017;46:5918-5929.

[40] Wang Y, Zhang L, Zhang G, Wu Y, Wu S, Yu J, Wang L. A new colorimetric and fluorescent bifunctional probe for Cu^{2+} and F^{-} ions based on perylene bisimide derivatives. Tetrahedron Lett 2014;55:3218-3222.

[41] Mishra R, Lim JM, Son M, Panini P, Kim D, Sankar J. Tuning the Electronic Nature of Mono□Bay Alkynyl–Phenyl□Substituted Perylene Bisimides: Synthesis, Structure, and Photophysical Properties. Chem Eur J 2014;20:5776-5786.

[42] Tan Y, Zhao Z, Shang L, Liu Y, Wei C, Li J, Wei H, Liu Z, Bian Z, Huang C. A novel bipolar D–π–A type phenanthroimidazole/carbazole hybrid material for high efficiency nondoped deep-blue organic light-emitting diodes with NTSC CIEy and low efficiency roll-off. J Mater Chem C, 2017;5:11901-11909.

[43] Schab-Balcerzak E, Iwan A, Grucela-Zajac M, Krompiec M, Podgorna M, Domanski M, Siwy M, Janeczek H. Characterization, liquid crystalline behavior, optical and electrochemical study of new aliphatic–aromatic polyimide with naphthalene and perylene subunits. Synth Met 2011;161:1660-1670.

[44] Zhou X, Sun Q, Li W, Zhao Y, Luo Z, Zhang F, Yang C. Isomeric small molecule acceptors based on perylene diimide and spirobifluorene for non-fullerene organic solar cells. Dyes Pigments 2017;146:151-158.

[45] Volpi G, Magnano G, Benesperi I, Saccone D, Priola E, Gianotti V, Milanesio M, Conterosito E, Barolo C, Viscardi G. One pot synthesis of low cost emitters with large Stokes' shift. Dyes Pigments 2017;137:152-164.

[46] Smolarek K, Ebenhoch B, Czechowski N, Prymaczek A, Twardowska M, Samuel IDW, Mackowski S. Silver nanowires enhance absorption of poly(3-hexylthiophene). Appl Phys Lett 2013;103:203302/1-4.

[47] Kotowicz S, Siwy M, Filapek M, Malecki JG, Smolarek K, Grzelak J, Mackowski S, Slodek A, Schab-Balcerzak E. New donor-acceptor-donor molecules based on quinolone acceptor unit with Schiff base bridge: synthesis and characterization. J Lumin 2017;183:458-469.

[48] Bujak P, Kulszewicz-Bajer I, Zagorska M, Maurel V, Wielgusa I, Pron A. Polymers for electronics and spintronics. Chem Soc Rev 2013;42:8895-8999.

[49] Kung Y-C, Hsiao S-H. Solution-processable, high-Tg, ambipolar polyimide electrochromics bearing pyrenylamine units. J Mater Chem 2011;21:1746-1754.

[50] Filapek M, Matussek M, Szlapa A, Kula S, Pająk M. The influence of experimental conditions and intermolecular interaction on the band gap determination. Case study of

perylene diimide and carbazole-fluorene derivatives. Electrochim Acta 2016;216:449-456.

[51] Grucela-Zajac M, Filapek M, Skorka L, Gasiorowski J, Glowacki ED, Neugebauer H, Schab-Balcerzak E. Thermal, optical, electrochemical, and electrochromic characteristics of novel polyimides bearing the Acridine Yellow moiety. Mater Chem Phys 2012;137:221-234.

[52] Schmidt R, Oh JH, Sun Y-S, Deppisch M, Krause A-M, Radacki K, Braunschweig H, Konemann M, Erk P, Bao Z, Wurthner F. High-Performance Air-Stable n-Channel Organic Thin Film Transistors Based on Halogenated Perylene Bisimide Semiconductors. J Am Chem Soc 2009;131:6215-5228.

Highlights

- Three novel perylene diimide (PDI) derivatives with bulky aromatic moieties were synthesized.
- Photophysical properties of the obtained compounds were thoroughly studied and compared with DTF calculations.
- The effect of substituents in bay positions of PDIs derivatives on photophysical properties was discussed.
- The emission enhancement of perylene diimide derivatives was presented by incorporation of silver nanowires due to plasmonics enhancement.